

Crystal structure built from a GeO_6 - GeO_5 polyhedra network with high thermal stability: β - SrGe_2O_5

Christian A. Niedermeier,^{1,*} Jun-ichi Yamaura,² Jiazhen Wu,² Xinyi He,¹ Takayoshi Katase,¹
Hideo Hosono^{1,2} and Toshio Kamiya^{1,2}

¹Laboratory for Materials and Structures, Institute of Innovative Research, Tokyo Institute of Technology, 4259 Nagatsuta, Midori, Yokohama 226-8503, Japan

²Materials Research Center for Element Strategy, Tokyo Institute of Technology, 4259 Nagatsuta, Midori, Yokohama, 226-8503, Japan

*Corresponding author: c-niedermeier@mces.titech.ac.jp

Abstract: By tackling the challenge of extending transparent oxide semiconductors to Ge-based oxides, we have found a not-yet-reported crystal structure, named β - SrGe_2O_5 , which is composed of edge-sharing GeO_6 octahedra interconnected by GeO_5 bipyramids. Single crystals were successfully grown by the high-pressure flux method. β - SrGe_2O_5 has a band gap of 5.2 eV and a dispersive conduction band with an effective mass as small as 0.34 times the electron rest mass, which originates from the edge-sharing GeO_6 octahedra network. Although known compounds with octahedral GeO_6 coordination are commonly unstable at atmospheric pressure and elevated temperatures, β - SrGe_2O_5 exhibits thermal stability up to 700 °C.

Transparent conducting oxides (TCOs) and transparent oxide semiconductors (TOS) are emerging materials combining electrical conductivity and high optical transparency in the visible spectral region, which find important applications in optoelectronic devices. In particular, semiconductors with a band gap in the ultraviolet spectral region are increasingly gaining relevance for power electronics as they can tolerate high electric fields without device failure. Conventionally, TOS compounds contain post-transition metal cations such as Zn^{2+} , In^{3+} and Sn^{4+} of $(n-1)d^{10}ns^0$ electronic configurations (n is the principal quantum number and should be ≥ 4)^{1,2}. Due to the wide spherical spread and overlap of the metal ns orbitals, an electron conduction path is formed³, which results in a dispersive conduction band (CB) and small effective mass. Main constituents of TOS had been limited to the above heavy cations, and the extension of materials systems is a challenging task with great importance for further developing the current state of electronics technology.

In comparison with Zn^{2+} , In^{3+} and Sn^{4+} , the effective ionic radius of Ge^{4+} is rather small, and therefore, Ge-based TOS had not been known until the discovery of the large band dispersion and the high electrical conductivity in the cubic perovskite $SrGeO_3$ (space group $Pm-3m$)⁴. In its network of corner-sharing, regular GeO_6 octahedra, the Ge^{4+} ions are 6-fold coordinated to O^{2-} ions. This high symmetry configuration prohibits the hybridization of Ge 4s and O 2p orbitals at the Γ point in the Brillouin zone, which forms the CB with exclusively Ge 4s non-bonding character and results in an exceptionally narrow 2.7 eV band gap and the first finding of high-density free electron doping in a Ge-based oxide. However, Ge^{4+} typically occupies the 4-fold coordinated tetrahedral sites in the majority of Ge oxides that are thermodynamically stable at ambient conditions. On the other hand, compounds in which all Ge^{4+} ions occupy 6-fold coordinated octahedral sites are rather exotic and commonly stable only in high pressure phases like the cubic perovskite $SrGeO_3$.

A recent high pressure study at 6 GPa reported α - $SrGe_2O_5$ (orthorhombic, $Cmca$), which crystal structure is built of stacked Ge oxide layers with corner-sharing GeO_6 octahedra and GeO_4 tetrahedra⁵. While the electrical properties and the electronic structure have not been reported, it may be expected that the separation of the Ge oxide layers in this structure and the large interatomic Ge-Ge distance due to the corner-sharing GeO_4 - GeO_6 network impedes the electron

transport. In contrast, the cubic perovskite SrGeO₃ is a very promising TCO, but the high synthesis pressure of 5 GPa⁶ and the low thermal stability⁷ are the key obstacles for practical applications. In particular, the crystalline-to-amorphous transition in cubic SrGeO₃ occurs at temperatures as low as 100 °C⁸. We thus target the synthesis of thermodynamically stable compounds built from a dense GeO₆ octahedral network, which would present very interesting novel candidates for high-mobility TOS.

In this paper, we report the discovery of a new crystal structure, named β -SrGe₂O₅ (orthorhombic, *Pnma*), with Ge ions in both 5-fold bipyramidal and 6-fold octahedral coordinations to O ions. This crystal structure is previously unknown and does not have any analogue in other material systems. According to density functional theory (DFT) calculations, β -SrGe₂O₅ is thermodynamically stable already at 1.4 GPa pressure, and the experiment confirms the good thermal stability up to 700 °C.

To find new Ge-based TOS, we inspected Ge-rich compounds of alkaline earth germanates as an analogue to the cubic perovskite SrGeO₃. Exploration of these materials for electronics is exciting due to two very advantageous features as compared to established TOS. First, the 1115 °C melting point of GeO₂ (trigonal, *P3₁21*) is remarkably low as compared to the neighboring group IV oxides such as SiO₂ (1710 °C), SnO₂ (>2100 °C⁹) and β -Ga₂O₃ (1820 °C¹⁰). The low melting temperature makes single crystal growth from the melt significantly easier. Secondly, the alkaline earth cations in such ionic-covalent mixed bonding compounds work as network modifiers which facilitate the design of the GeO_x polyhedra linkage and the Ge coordination.

Surprisingly, the ambient-pressure CaO-GeO₂ phase diagram¹¹ (Fig. S1(a)¹²) shows the stability of CaGe₂O₅ (monoclinic, *C2/c*), which is composed of a corner-connected GeO₄-GeO₆ network¹³, whereas the compositional analogue of SrGe₂O₅ is not known¹⁴ and solely the high-pressure α -SrGe₂O₅ (orthorhombic, *Cmca*) phase has been synthesized at 6 GPa⁵. To find a dense crystal structure built from a network of GeO₆ octahedra, we investigated the Ge-rich part of the SrO-GeO₂ using differential thermal analysis (DTA). Remarkably, the compounds SrGeO₃ (monoclinic, *C2/c*) and SrGe₄O₉ (trigonal, *P321*) show a low 1164 °C eutectic temperature, while the SrGe₂O₅ phase is not observed (Fig. S1(b)).

We thus turned to investigate the stability of a dense SrGe₂O₅ phase at elevated pressure

conditions. Applying the high-pressure synthesis and a SrCl₂/NaCl flux, we obtained colorless SrGe₂O₅ single crystals of up to 0.4 x 0.3 x 0.3 mm³ size (Fig. 1(a)). We performed single crystal X-ray diffraction (XRD) measurement of the SrGe₂O₅ sample at room temperature. The initial structural model (orthorhombic, *Pmna*), named β -SrGe₂O₅, was suggested based on the unit cell dimensions and the reflection data. The final crystallographic parameters are listed in Table 1. The internal atomic coordinates, displacement parameters, and the displacement ellipsoid structure are given in Tables S1 and S2, and Fig. S2, respectively. The Rietveld refinement of the Bragg-Brentano powder XRD pattern of ground single crystals is well converged using the determined β -SrGe₂O₅ crystal structure (Fig. 1(b)), guaranteeing the phase stability after the grinding process.

Table 1: Crystallographic parameters for β -SrGe₂O₅.

Chemical formula	SrGe ₂ O ₅
Crystal system	Orthorhombic
Space group	<i>Pmna</i> (#62)
Temperature (K)	296
Density, calc. (g/cm ³)	5.65
Unit cell volume (Å ³)	368.001(15)
Lattice parameters <i>a</i> , <i>b</i> , <i>c</i> (Å)	6.7530(2), 5.8725(1), 9.2796(2)
Calc. lattice parameters <i>a</i> , <i>b</i> , <i>c</i> (Å) ^a	6.7303, 5.8748, 9.2990
Crystal size (μm ³)	70 x 50 x 50
Radiation source	Mo K _α
Absorption correction	Numerical, NUMABS ¹⁵
No. of measured reflections	10264
No. of independent reflections	1398
R _{int} ^b	0.052
(sin θ/λ) _{max} (Å ⁻¹)	0.5
R ₁ [F ² > 2σ(F ²)], wR ₂ (F ²), S ^b	0.049, 0.146, 1.13
No. of parameters	47
Δρ _{max} , Δρ _{min} (eÅ ⁻³)	2.93, -2.55

^aObtained by hybrid DFT calculation using the PBE0 functional.

^bSee the SHELX manual¹⁶ for definition of the residual and goodness of fit factors.

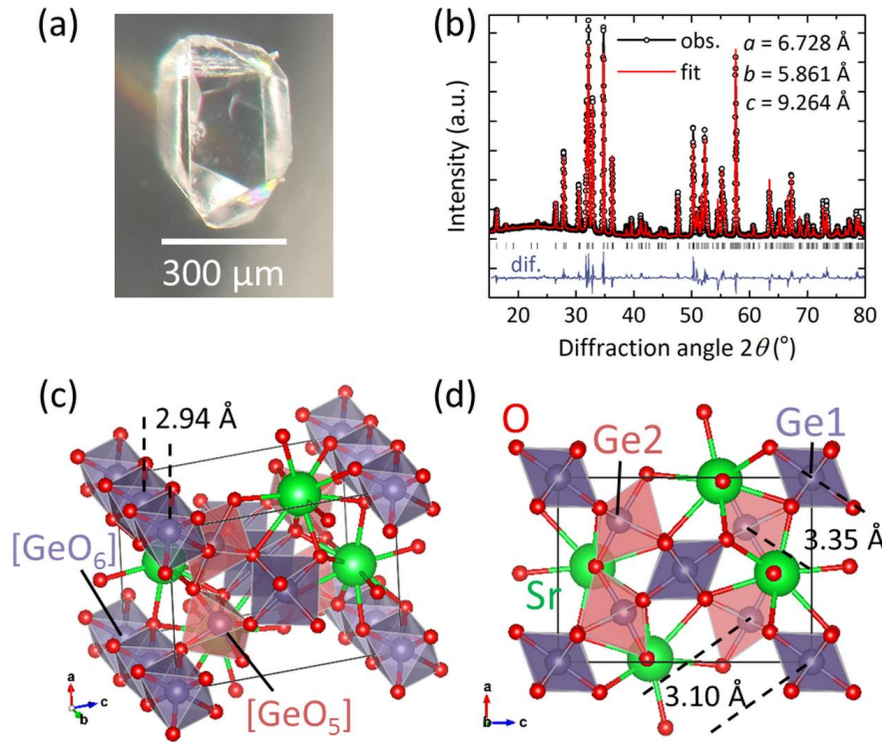


Fig. 1: (a) Optical micrograph of a transparent β - SrGe_2O_5 single crystal. (b) Bragg-Brentano powder XRD pattern of ground β - SrGe_2O_5 single crystals (black data points) with the result of Rietveld refinement (red line). (c,d) The β - SrGe_2O_5 (orthorhombic, $Pnma$) crystal structure with 5-fold and 6-fold coordinated Ge indicated by the red and purple polyhedra, respectively.

The crystal structure of β - SrGe_2O_5 , which has an orthorhombic lattice and belongs to the $Pnma$ space group, is illustrated in Figs. 1(c) and 1(d). The Sr^{2+} ion is 10-fold coordinated to the surrounding O^{2-} ions. The GeO_6 octahedra form edge-sharing one-dimensional chains along the b-axis. These GeO_6 chains are further corner-linked to GeO_5 triangular bipyramids, resulting in a three-dimensional cross-linked network with GeO_5 - GeO_6 chains along the $[1-11]$ and $[11-1]$ crystallographic directions. The Ge-O bond lengths and O-Ge-O bond angles in the GeO_6 octahedron are 1.88–1.96 Å and 80.7–99.3°, indicating a minor distortion. The present phase shows some structural similarity to CaGe_2O_5 (orthorhombic, $Pbam$) obtained at 8 GPa pressure¹⁷, in which Ge is 5- and 6-fold coordinated on square pyramidal and octahedral sites, respectively. In CaGe_2O_5 , the degree of GeO_6 octahedral distortion is similar to that in β - SrGe_2O_5 , showing Ge-O bond lengths and O-Ge-O bond angles of 1.87–1.94 Å and 82.4–97.3°, respectively. In α -

SrGe₂O₅ (orthorhombic, *Cmca*), the Ge-O bond lengths are spread most widely from 1.84–1.99 Å. The detailed comparison of the Ge-O bond lengths and O-Ge-O bond angles in these structures, with reference to the high-symmetry cubic SrGeO₃ perovskite, is summarized in Fig. S3.

The interatomic Ge-Ge distance between the corner-linked GeO₆ octahedra in cubic SrGeO₃ of 3.80 Å is significantly larger than that of the edge-sharing GeO₆ octahedra in β -SrGe₂O₅ (2.94 Å) and CaGe₂O₅ (orthorhombic, *Pbam*) (2.82 Å). The Ge1-Ge2 interatomic distances within the corner-sharing GeO₅-GeO₆ polyhedral chains in β -SrGe₂O₅ are 3.10 Å and 3.35 Å (Fig. 1(d)), which are slightly longer than those between the edge-sharing GeO₆ octahedra. In CaGe₂O₅, the analogous Ge1-Ge2 distances are longer (3.36 Å and 3.43 Å), despite the smaller Ca²⁺ effective ionic radius as compared to Sr²⁺. In general, a small interatomic distance between the Ge4s orbitals, which form the CB, is beneficial for forming a high-mobility electron conduction path due to larger overlaps³. In the case of cubic SrGeO₃, however, the coordination symmetry is the key factor for determining the electron transport since the conduction path is formed by a Ge-O non-bonding state at the Γ point and Ge-O anti-bonding states at the Brillouin zone boundaries^{18,19}. The Ge-O-Ge bond angle between two GeO₆ octahedra is exactly 180° which presents the largest possible interatomic distance of two Ge atoms in the network of GeO₆ octahedra.

Hybrid DFT calculations using the PBE0 functional²⁰ were performed to obtain the β -SrGe₂O₅ (orthorhombic, *Pnma*) ground state crystal structure. The lattice parameters are 6.73, 5.87 and 9.30 Å, which is within 0.4% relative error compared to the experimental values at room temperature (Table 1). The β -SrGe₂O₅ electronic band structure shows a 5.17 eV indirect band gap, with the CB minimum located at the Γ point and the valence band (VB) maximum located at the T [0 1/2 1/2] point of the Brillouin zone (Fig. 2(a)). The CB is dominated by Ge 4s and O 2p states, while the VB is mainly comprised of O 2p states (Fig. 2(b)). The β -SrGe₂O₅ CB is dispersive around the Γ point, with an effective mass as small as 0.34 times the electron rest mass m_e in the Γ -Y direction (Table S3). The large dispersion along this direction is thus attributed to the chain of edge-sharing GeO₆ octahedra along the b-axis. The value of the effective mass is comparable to 0.28 m_e for the prototype TCO SnO₂²¹, which is also built of edge- and corner-sharing SnO₆ octahedra, similar to β -SrGe₂O₅.

We measured the reflection ellipsometry spectrum from 0.6–5.2 eV photon energy for a mirror-polished β -SrGe₂O₅ polycrystalline pellet. The steep increase in the real ϵ_1 and imaginary part ϵ_2 of the dielectric function approaching 5.2 eV energy is consistent with the calculated 5.20 eV direct electronic band gap (Fig. 2(c)). Using density functional perturbation theory²², the frequency-dependent real and imaginary dielectric tensor elements ϵ_x , ϵ_y and ϵ_z are calculated and their averages are given for comparison.

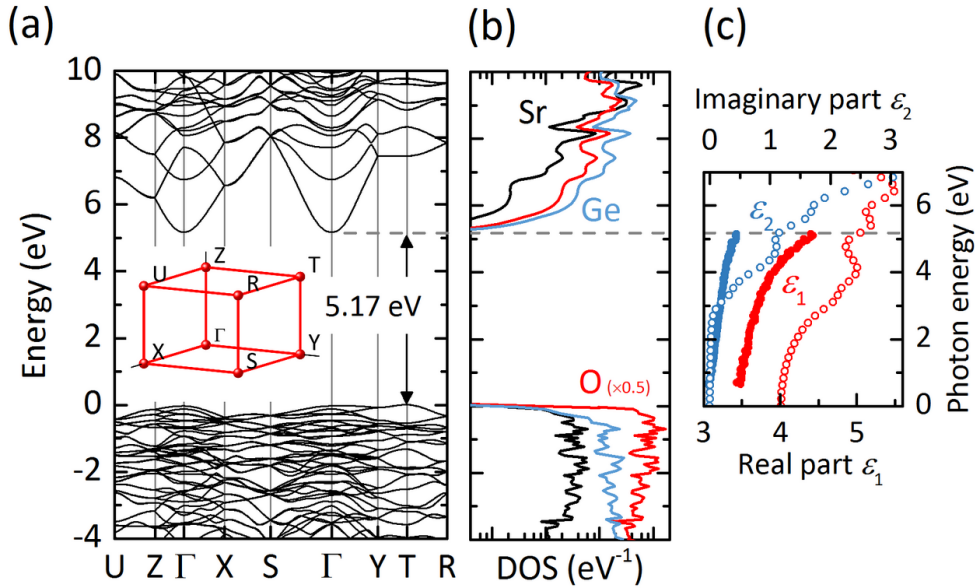


Fig. 2: (a) PBE0 band structure along high symmetry directions in the first Brillouin zone indicates a large CB dispersion and a 5.17 eV indirect band gap. (b) The density of states (DOS) in logarithmic scale shows that the CB is derived from Ge and O states while mainly O states contribute to the VB. (c) The measured real ϵ_1 and imaginary part ϵ_2 of the dielectric function of a mirror-polished β -SrGe₂O₅ polycrystalline pellet is given by the filled circles. For comparison, the averages of the calculated real and imaginary dielectric tensor elements ϵ_x , ϵ_y and ϵ_z are given by the open circles.

To assess the eligibility as TOS and investigate electrical properties, we doped Sb to substitute Ge in β -SrGe₂O₅ single crystals and β -Sr(Ge_{0.95}Sb_{0.05})₂O₅ polycrystalline pellets. The Sb-doped β -SrGe₂O₅ single crystals show a dark blue color, but the polycrystalline pellets are electrically insulating and free carriers cannot be detected in the infrared reflectance spectrum (Fig. S4). The efficient impurity doping and underlying compensation mechanisms shall be the subject of

further investigation.

Since compounds with octahedral GeO₆ coordination are commonly unstable in particular at atmospheric pressure, we investigate the β -SrGe₂O₅ thermodynamic stability theoretically using DFT calculations. The calculated formation enthalpy

$$\Delta H_f^{\text{SrGe}_2\text{O}_5} = \mu_{\text{Sr}} + 2\mu_{\text{Ge}} + 5\mu_{\text{O}} \quad (1)$$

is constrained by the chemical potentials μ of elemental Sr, Ge and molecular O₂, with the origins at zero pressure and absolute zero temperature. The equilibrium conditions to prevent precipitation into solid elemental Sr (cubic, *Fm-3m*), Ge (cubic, *Fd-3m*) and molecular O₂, $\mu_{\text{Sr}} \leq 0$, $\mu_{\text{Ge}} \leq 0$ and $\mu_{\text{O}} \leq 0$ define the stable potential window boundaries. Considering all known phases in the quasi-binary SrO-GeO₂ system, including SrO (cubic, *Fm-3m*) and Sr₂GeO₄ (orthorhombic, *Pna2₁*), the most stable phases are determined within the given potential range. For zero external pressure, we confirm that the β -SrGe₂O₅ phase is not thermodynamically stable under equilibrium (Fig. 3(a)).

To investigate the β -SrGe₂O₅ stability at elevated pressures, the energy calculations of all (meta)stable compounds, including the high-pressure polymorphs in the SrO-GeO₂ system, were performed for a fixed set of volumes around the equilibrium volume (Fig. S5, Table S5). The Murnaghan equation²³ was used to derive an equation of state for fitting of the obtained energy-volume curves and the formation enthalpy is derived as a function of pressure¹². Already at pressures as low as 2 GPa, a β -SrGe₂O₅ potential window is obtained with phase boundaries to SrGeO₃ (triclinic, *P-1*) and GeO₂ (tetragonal, *P4₂/mnm*) (Fig. 3(b)).

The transition pressure for the β -SrGe₂O₅ formation is determined by comparison with the enthalpy of the decomposition products, SrGeO₃ + GeO₂. The decomposition is energetically favored only for pressures below 1.4 GPa (Fig. 3(c)). Since the enthalpy difference between β -SrGe₂O₅ and the decomposition products at zero pressure is only about 0.01 eV/atom, it shall be possible to synthesize β -SrGe₂O₅ at ambient pressure under optimized growth conditions. For example, providing a crystal seed or epitaxial template favorable for the nucleation and growth of β -SrGe₂O₅ may realize such conditions. Moreover, the calculation shows that β -SrGe₂O₅ is the most stable modification at ambient pressure in comparison with the high-pressure α -SrGe₂O₅ (orthorhombic, *Cmca*) phase obtained at 6 GPa⁵.

To investigate the thermal stability of β -SrGe₂O₅, the single crystals were ground to powder and annealed in air at ambient pressure. After thermal annealing of β -SrGe₂O₅ at 700 °C for 1 h, the XRD pattern shows that the phase remains stable and decomposition into SrGeO₃, SrGe₄O₉ and GeO₂ occurs only at elevated temperatures (Fig. 3(d)). The thermal stability facilitates growth of single crystals at ambient pressure through a suitable flux by adding a seed crystal when cooling from 700 °C temperature.

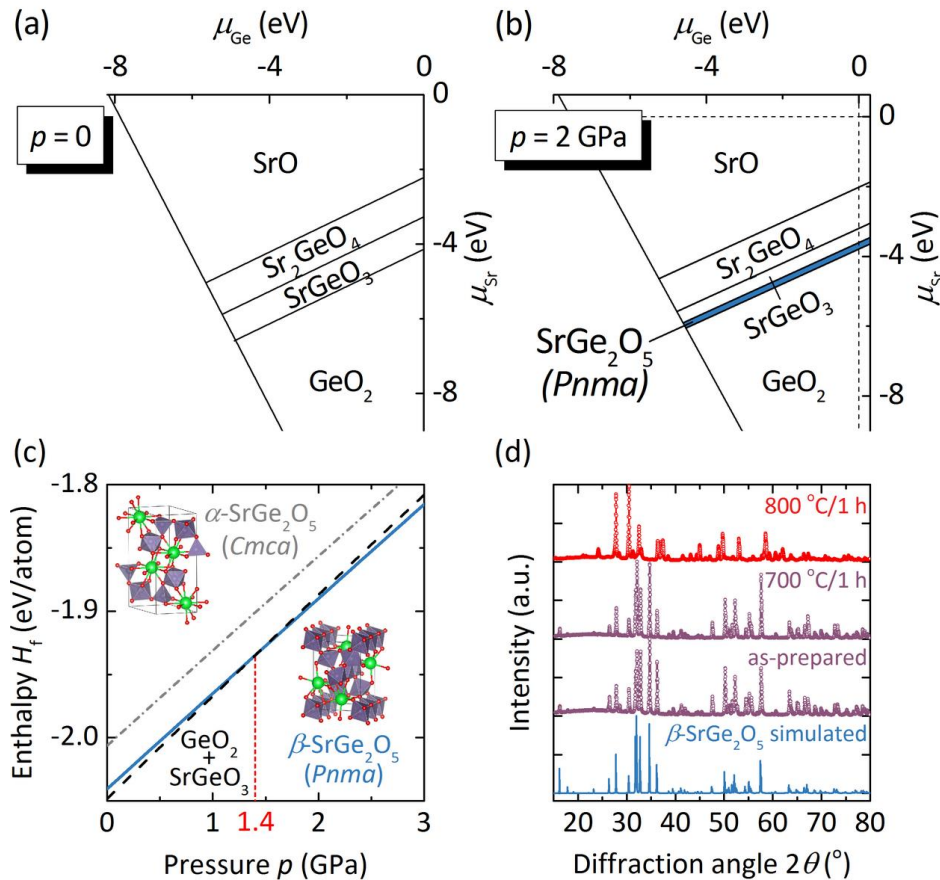


Fig. 3: (a) Absence of a chemical potential window for β -SrGe₂O₅ at zero pressure shows that the phase is not thermodynamically stable at the standard condition. (b) At a pressure as low as 2 GPa, β -SrGe₂O₅ becomes stable within the chemical potential window indicated by the blue area. (c) Formation of a phase-separated SrGeO₃-GeO₂ system is energetically favored over β -SrGe₂O₅ only for pressures below 1.4 GPa. (d) Bragg-Brentano XRD patterns of ground and annealed single crystals confirm the thermal stability of β -SrGe₂O₅ up to 700 °C temperature.

In summary, we have discovered a previously unknown crystal structure, orthorhombic β -SrGe₂O₅ which belongs to the *Pnma* space group. The single crystals were successfully grown using the high-pressure flux method. β -SrGe₂O₅ has a band gap of 5.2 eV and shows a large CB dispersion with an effective mass as small as 0.34 m_e as a result of the edge-sharing GeO₆ octahedral network. The calculated pressure required for the β -SrGe₂O₅ synthesis is only about 1.4 GPa and the material shows good thermal stability at temperatures up to 700 °C.

Supporting Information

CaO-GeO₂ and SrO-GeO₂ phase diagrams, β -SrGe₂O₅ crystallographic information, calculated effective mass along different symmetry directions, characterization of Sb-doped β -SrGe₂O₅, enthalpy equation of state for compounds in the SrO-GeO₂ system as a function of pressure, experimental and computational methods.

Acknowledgements

The work at Tokyo Institute of Technology was supported by the MEXT Element Strategy Initiative to Form Core Research Center. C.A.N. acknowledges the support through a fellowship granted by the German Research Foundation (DFG) for proposal NI1834.

References

- (1) Hosono, H.; Kikuchi, N.; Ueda, N.; Kawazoe, H. Working Hypothesis to Explore Novel Wide Band Gap Electrically Conducting Amorphous Oxides and Examples. *J. Non. Cryst. Solids* **1996**, *198–200*, 165. [https://doi.org/http://dx.doi.org/10.1016/0022-3093\(96\)80019-6](https://doi.org/http://dx.doi.org/10.1016/0022-3093(96)80019-6).
- (2) Kawazoe, H.; Yanagi, H.; Ueda, K.; Hosono, H. Transparent *p*-Type Conducting Oxides: Design and Fabrication of *p-n* Heterojunctions. *MRS Bull.* **2000**, *25* (8), 28–36. <https://doi.org/10.1557/mrs2000.148>.
- (3) Hosono, H.; Ueda, K. Transparent Conductive Oxides. In *Springer Handbook of Electronic*

- and Photonic Materials*; Kasap, S., Capper, P., Eds.; Springer International Publishing: Cham, 2017; p 1. https://doi.org/10.1007/978-3-319-48933-9_58.
- (4) Mizoguchi, H.; Kamiya, T.; Matsuishi, S.; Hosono, H. A Germanate Transparent Conductive Oxide. *Nat. Commun.* **2011**, *2*, 470.
 - (5) Nakatsuka, A.; Sugiyama, K.; Ohkawa, M.; Ohtaka, O.; Fujiwara, K.; Yoshiasa, A. A New High-Pressure Strontium Germanate, SrGe₂O₅. *Acta Crystallogr. Sect. C* **2016**, *72*, 716. <https://doi.org/10.1107/S205322961601353X>.
 - (6) Shimizu, Y.; Syono, Y.; Akimoto, S. High-Pressure Transformations in SrGeO₃, SrSiO₃, BaGeO₃, and BaSiO₃. *High Temp. High Press.* **1970**, *2*, 113.
 - (7) Andraut, D.; Itie, J.; Farges, F. High-Temperature Structural Study of Germanate Perovskites and Pyroxenoids. *Am. Mineral.* **1996**, *81*, 822.
 - (8) Nakatsuka, A.; Yoshiasa, A.; Fujiwara, K.; Ohtaka, O. Variable-Temperature Single-Crystal X-Ray Diffraction Study of SrGeO₃ High-Pressure Perovskite Phase. *J. Mineral. Petrol. Sci.* **2018**, *113*, 280. <https://doi.org/10.2465/jmps.180605>.
 - (9) Galazka, Z.; Uecker, R.; Klimm, D.; Irmscher, K.; Pietsch, M.; Schewski, R.; Albrecht, M.; Kwasniewski, A.; Ganschow, S.; Schulz, D.; et al. Growth, Characterization, and Properties of Bulk SnO₂ Single Crystals. *Phys. status solidi* **2014**, *211*, 66.
 - (10) Galazka, Z. Growth Measures to Achieve Bulk Single Crystals of Transparent Semiconducting and Conducting Oxides. *Handb. Cryst. Growth* **2015**, 209–240. <https://doi.org/10.1016/B978-0-444-63303-3.00006-7>.
 - (11) Shirvinskaya, A. K.; Grebenshchikov, R. G.; Toropov, N. A. -. *Inorg. Mater.* **1966**, *2*, 286.
 - (12) See Supplementary Material at [Url] for CaO-GeO₂ and SrO-GeO₂ Phase Diagrams, Beta-SrGe₂O₅ Crystallographic Information, Calculated Effective Mass along Different Symmetry Directions, Sb-Doped Beta-SrGe₂O₅ Single Crystal and IR Reflectance, Enthalpy Equat.
 - (13) Malcherek, T.; Bosenick, A. Structure and Phase Transition of CaGe₂O₅ Revisited. *Phys. Chem. Miner.* **2004**, *31*, 224. <https://doi.org/10.1007/s00269-003-0364-9>.

- (14) Grebenschikov, R. G.; Shirvinskaya, A. K.; Parfenenkov, V. N.; Shitova, V. I.; Toropov, N. A. СИСТЕМА Окись СТРОНЦИЯ - ДВУОКИСЬ ГЕРМАНИЯ. *Dokl. Akad. Nauk SSSR* **1967**, *174*, 839.
- (15) T. Higashi, NUMABS, Rigaku Corporation, Tokyo, Japan. NUMABS, Rigaku Corporation, Tokyo, Japan. *Rigaku Corporation, Tokyo, Japan*. 1995.
- (16) [Http://shelx.uni-goettingen.de/shelx97.pdf](http://shelx.uni-goettingen.de/shelx97.pdf). SHELX-97 manual <http://shelx.uni-goettingen.de/shelx97.pdf> (accessed Jul 24, 2019).
- (17) Nemeth, P.; Buseck, P. R.; Leinenweber, K.; Groy, T. L. A New High-Pressure CaGe₂O₅ Polymorph with 5- and 6-Coordinated Germanium. *Am. Mineral.* **2007**, *92*, 441.
- (18) Highbanks, T. Superdegenerate Electronic Energy Levels in Extended Structures. *J. Am. Chem. Soc.* **1985**, *107* (24), 6851–6859. <https://doi.org/10.1021/ja00310a018>.
- (19) Mizoguchi, H.; Woodward, P. M.; Byeon, S.-H.; Parise, J. B. Polymorphism in NaSbO₃: Structure and Bonding in Metal Oxides. *J. Am. Chem. Soc.* **2004**, *126* (10), 3175–3184. <https://doi.org/10.1021/ja038365h>.
- (20) Perdew, J. P.; Ernzerhof, M.; Burke, K. Rationale for Mixing Exact Exchange with Density Functional Approximations. *J. Chem. Phys.* **1996**, *105* (22), 9982–9985. <https://doi.org/10.1063/1.472933>.
- (21) Button, K. J.; Fonstad, C. G.; Dreybrodt, W. Determination of the Electron Masses in Stannic Oxide by Submillimeter Cyclotron Resonance. *Phys. Rev. B* **1971**, *4* (12), 4539. <https://doi.org/10.1103/PhysRevB.4.4539>.
- (22) Gajdoš, M.; Hummer, K.; Kresse, G.; Furthmüller, J.; Bechstedt, F. Linear Optical Properties in the Projector-Augmented Wave Methodology. *Phys. Rev. B* **2006**, *73* (4), 45112. <https://doi.org/10.1103/PhysRevB.73.045112>.
- (23) Murnaghan, F. D. The Compressibility of Media under Extreme Pressures. *Proc. Natl. Acad. Sci.* **1944**, *30*, 244. <https://doi.org/10.1073/pnas.30.9.244>.

Supporting information for
Crystal structure built from a GeO₆-GeO₅ polyhedra network
with high thermal stability: β -SrGe₂O₅

Christian A. Niedermeier,^{1,*} Jun-ichi Yamaura,² Jiazhen Wu,² Xinyi He,¹ Takayoshi Katase,¹ Hideo Hosono^{1,2} and Toshio Kamiya^{1,2}

¹Laboratory for Materials and Structures, Institute of Innovative Research, Tokyo Institute of Technology, 4259 Nagatsuta, Midori, Yokohama 226-8503, Japan

²Materials Research Center for Element Strategy, Tokyo Institute of Technology, 4259 Nagatsuta, Midori, Yokohama, 226-8503, Japan

**Corresponding author: c-niedermeier@mces.titech.ac.jp*

CaO–GeO₂ and SrO–GeO₂ phase diagrams

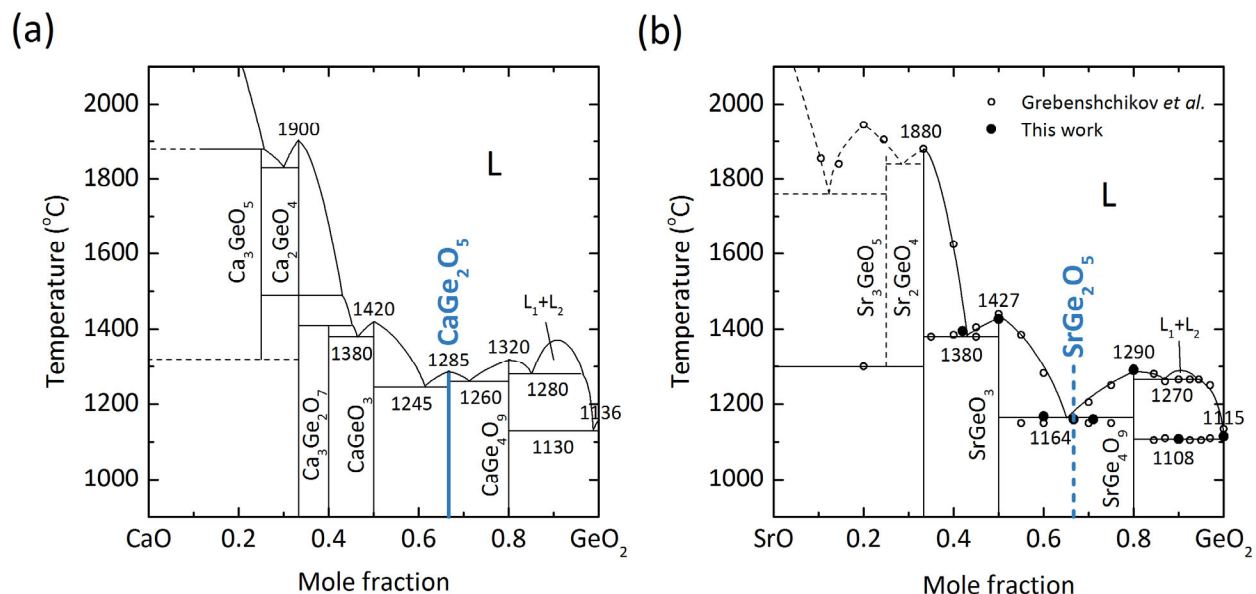


Fig. S1: (a) The CaO–GeO₂ phase diagram reprinted from Shirvinskaya *et al.*¹ indicates the existence of an ambient-pressure stable CaGe₂O₅ phase. (b) The SrO–GeO₂ phase diagram with the open data points is cited from Grebenshchikov *et al.*² In this reference, the Sr₃GeO₅ phase erroneously appears at a GeO₂ mole fraction of 0.2, which we corrected to 0.25 without experimental confirmation. The closed circles present our data obtained by DTA. The composition of SrGe₂O₅ is indicated with the blue dashed line.

β -SrGe₂O₅ Crystallographic Information

Table S1: Internal atomic coordinates x , y and z and equivalent isotropic displacement parameters U_{eq} (\AA^2) for β -SrGe₂O₅.

Atom	x	y	z	U_{eq}
Sr	0.9811(1)	0.75	0.63611(6)	0.0071(1)
Ge1	0.5	0.5	0.5	0.0040(1)
Ge2	0.7307(1)	0.25	0.74124(7)	0.0043(1)
O1	0.8430(7)	0.25	0.9194(5)	0.0057(6)
O2	0.6441(7)	0.25	0.4244(5)	0.0060(6)
O3	0.6630(5)	0.5141(6)	0.6635(3)	0.0063(5)
O4	0.9812(8)	0.25	0.6493(5)	0.0100(8)

Table S2: Atomic displacement parameters (ADP) in \AA^2 for β -SrGe₂O₅.

Atom	U^{11}	U^{22}	U^{33}	U^{12}	U^{13}	U^{23}
Sr	0.0062(2)	0.0095(2)	0.0056(2)	0	0.00021(15)	0
Ge1	0.0045(2)	0.0047(2)	0.0028(2)	0.00013(17)	-0.00050(15)	0.00015(17)
Ge2	0.0052(2)	0.0049(2)	0.0028(2)	0	-0.00107(16)	0
O1	0.0083(16)	0.0075(16)	0.0013(12)	0	-0.0020(11)	0
O2	0.0064(15)	0.0068(16)	0.0048(14)	0	0.0004(12)	0
O3	0.0092(11)	0.0045(11)	0.0053(10)	0.0010(9)	-0.0025(8)	0.0002(9)
O4	0.0057(16)	0.020(2)	0.0047(15)	0	0.0008(12)	0

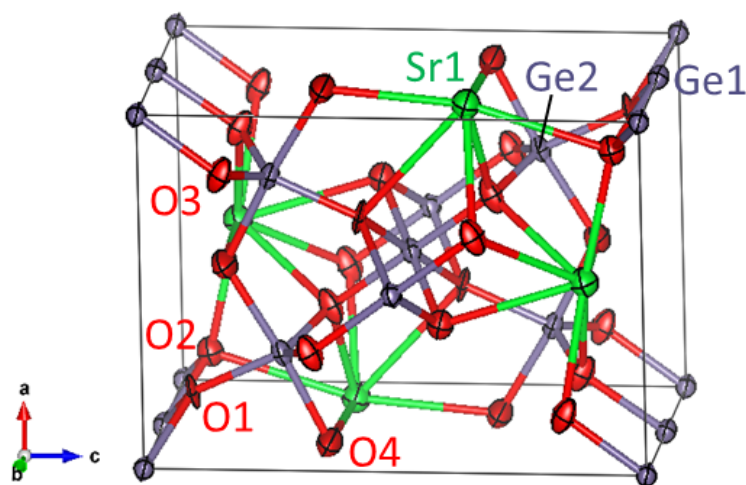


Fig. S2: β -SrGe₂O₅ crystal structure with internal atomic positions presented by displacement ellipsoids of 99% probability density as determined by the data in Tables S1 and S2.

Table S3: Comments on Level C alerts of the checkCIF/PLATON report for the structure refinement result of β -SrGe₂O₅.

Alert	Problem	Comment
DIFMX02 ALERT 1 C	The maximum difference density is $> 0.1 \cdot Z_{\text{MAX}} \cdot 0.75$. The relevant atom site should be identified.	The maximum difference density occurs near the Ge atoms.
PLAT097 ALERT 2 C	Large reported max. (positive) residual density, $3.08 \text{ e}\text{\AA}^{-3}$	The difference densities are located near the Sr and Ge atoms. These are ghost peaks which result from the difference Fourier synthesis.
PLAT213 ALERT 2 C	Atom O1 has ADP max/min ratio, 3.4 oblate	We checked its origin carefully, including the lowering of the symmetry.
PLAT250 ALERT 2 C	Large U3/U1 ratio for average U(i,j) tensor, 2.4 note	The O1 and O4 atoms indicate large ADP.

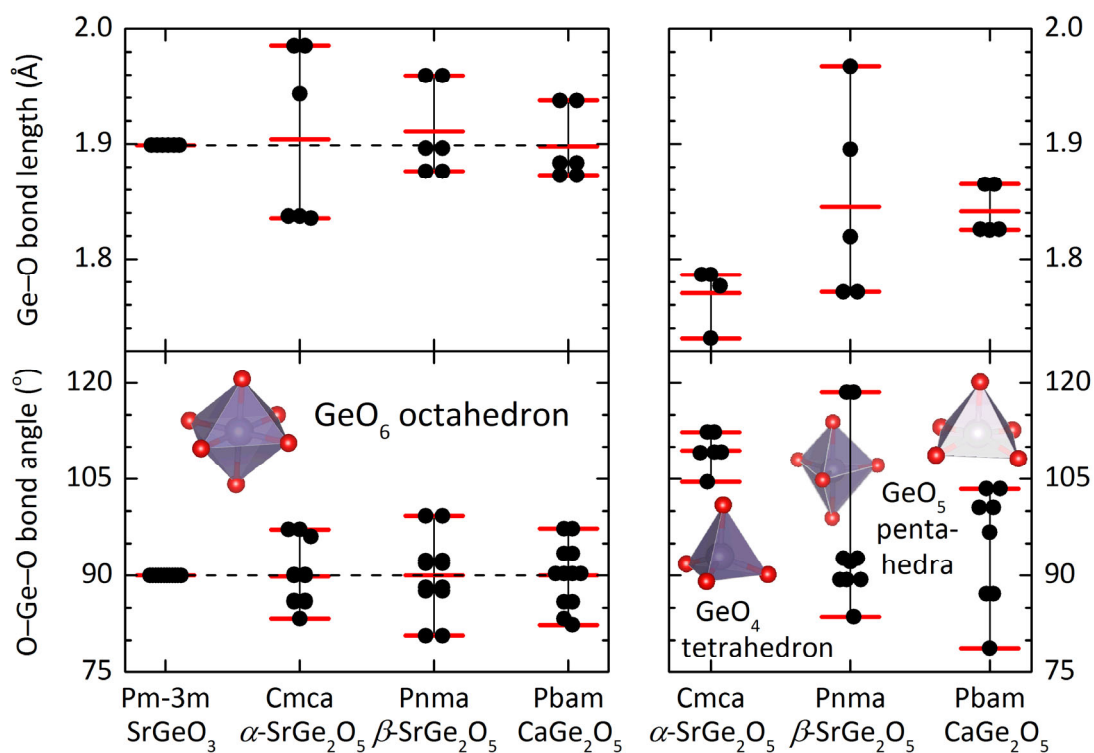


Fig. S3: Comparison of Ge-O bond lengths and O-Ge-O bond angles in the structures SrGeO₃ (cubic, *Pm-3m*),³ α -SrGe₂O₅ (orthorhombic, *Cmca*),⁴ β -SrGe₂O₅ (orthorhombic, *Pnma*) and CaGe₂O₅ (orthorhombic, *Pbam*)⁵ for the GeO₆ octahedron, and GeO₅ and GeO₄ polyhedra. Red bars denote maximum, mean and minimum values, respectively.

Calculation of the Effective Mass

Using the calculated band structure, the effective mass (Table S3) is determined from the CB curvature at the Γ point⁶

$$m_e^* = \hbar^2 \left(\frac{d^2 E}{dk^2} \right)^{-1} \quad (1)$$

where \hbar is the reduced Planck constant and k is the reciprocal space vector.

Table S4: Effective mass m_e^* (in units of the electron rest mass m_e) along high symmetry directions in the first Brillouin zone of β -SrGe₂O₅ obtained using the PBE0 hybrid functional.

Symmetry direction	m_e^*/m_e
Γ -X	0.42
Γ -Y	0.34
Γ -Z	0.37
Γ -S	0.40

Sb-doping of β -SrGe₂O₅ and IR Reflectance

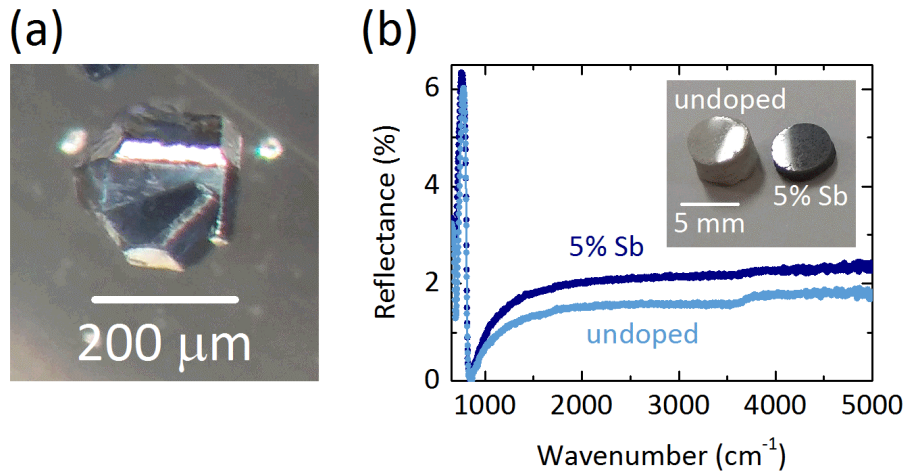


Fig. S4: (a) Optical micrograph of Sb-doped β -SrGe₂O₅ single crystal. (b) IR reflectivity spectrum of undoped β -SrGe₂O₅ and Sr(Ge_{0.95}Sb_{0.05})₂O₅ polycrystalline pellets indicating that the reflectance edge at a wavenumber of 820 cm⁻¹ does not shift with Sb doping.

The Enthalpy Equation of State

The Murnaghan equation is derived from the approximation that the bulk modulus of a material follows a linear dependence on pressure p at constant temperature T ⁷

$$-V \left(\frac{\partial p}{\partial V} \right)_T = K_0 + K_1 p \quad (2)$$

The constants K_0 and K_1 denote the bulk modulus at zero pressure and the first derivative thereof, respectively. The Murnaghan equation is obtained after integrating Eq. (2), which yields the dependence of volume V with respect to the equilibrium volume V_0 at zero pressure as a function of pressure p

$$\frac{V}{V_0} = \left(1 + \frac{K_1}{K_0} p \right)^{-\frac{1}{K_1}} \quad (3)$$

Rearranging yields

$$p = \frac{K_0}{K_1} \left[\left(\frac{V_0}{V} \right)^{K_1} - 1 \right] \quad (4)$$

The pressure p is given by the derivation of energy E after volume V at constant entropy S ⁸

$$p = - \left(\frac{\partial E}{\partial V} \right)_S \quad (5)$$

Inserting into Eq. (4), and integrating, yields the equation of state for the energy E as a function of volume V

$$E = E_0 + \frac{K_0}{K_1} V \left[\left(\frac{V_0}{V} \right)^{K_1} \frac{1}{K_1 - 1} + 1 \right] - \frac{K_0 V_0}{K_1 - 1} \quad (6)$$

Here, E_0 denotes the equilibrium energy at zero pressure. The enthalpy H is calculated according to⁸

$$H = E + pV \quad (7)$$

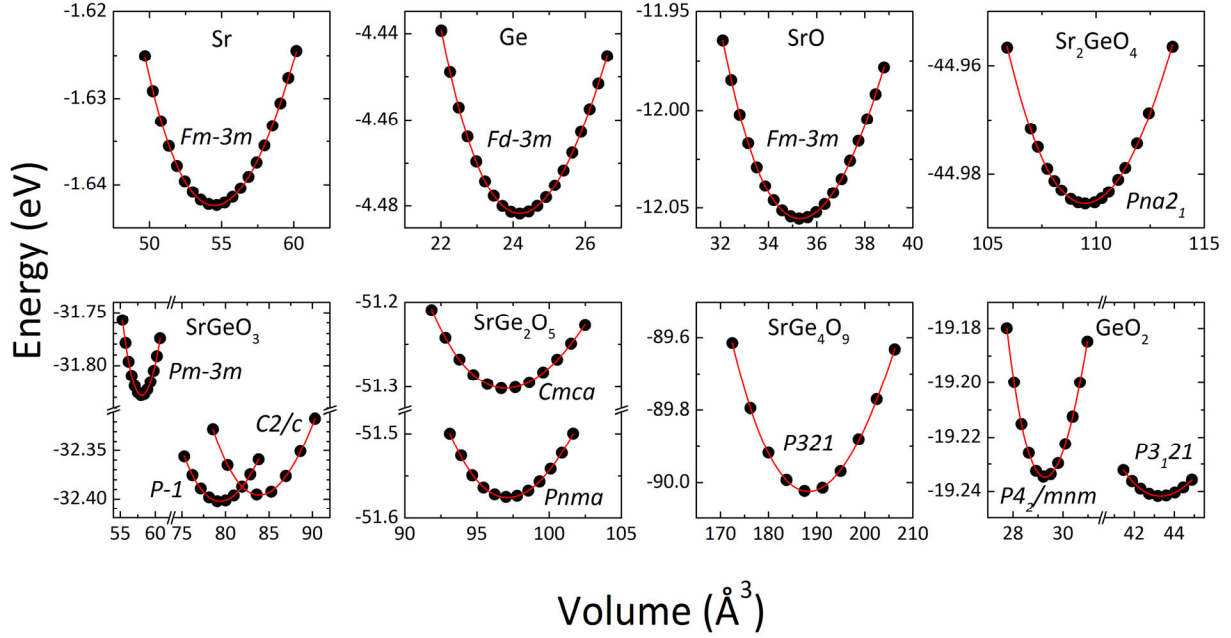


Fig. S5: PBE-calculated energy-volume dependence of elemental Sr, Ge and compounds in the SrO-GeO₂ system. Equilibrium energy E_0 and volume V_0 are given per unit formula. The red lines show fitting curves using the Murnaghan equation of state (Eq. (6)).

Table S5: Murnaghan equation of state (Eq. (6)) parameters for elemental Sr, Ge, and compounds in the SrO-GeO₂ system. Equilibrium energy E_0 and volume V_0 are given per unit formula. K_0 and K_1 denote the bulk modulus at zero pressure and the first derivative thereof, respectively.

Material	Crystal system	Space group	E_0 (eV)	V_0 (Å ³)	K_0 (GPa)	K_1 -
Sr	cubic	<i>Fm-3m</i>	-1.64	54.51	11.3	3.47
Ge	cubic	<i>Fd-3m</i>	-4.48	24.19	57.9	4.71
SrO	cubic	<i>Fm-3m</i>	-12.06	35.31	84.4	4.36
Sr ₂ GeO ₄	orthorhombic	<i>Pna2₁</i>	-44.99	109.49	71.0	8.52
SrGeO ₃	monoclinic	<i>C2/c</i>	-32.40	83.88	58.4	4.20
	triclinic	<i>P-1</i>	-32.40	79.40	63.4	4.75
	cubic	<i>Pm-3m</i>	-31.83	58.06	157.3	5.10
SrGe ₂ O ₅	orthorhombic	<i>Pnma</i>	-51.58	97.13	129.3	7.70
	orthorhombic	<i>Cmca</i>	-51.30	96.99	91.3	8.70
SrGe ₄ O ₉	trigonal	<i>P321</i>	-90.02	188.34	85.5	3.81
GeO ₂	trigonal	<i>P3₁21</i>	-19.24	43.31	35.90	3.87
	tetragonal	<i>P4₂/mnm</i>	-19.23	29.29	190.5	6.86

Experimental Methods

We prepared $(\text{SrO})_{1-x}(\text{GeO}_2)_x$ compounds and two-phase mixtures with the compositions $0.42 \leq x \leq 1$ by calcination of SrCO_3 and GeO_2 in stoichiometric quantities at 950–1100 °C for 12 h. The melting points and eutectic temperatures were determined by using differential thermal analysis (Bruker TG-DTA 2020SA) up to 1450 °C. A Pt crucible filled with Al_2O_3 powder was used as a heat transfer reference.

To grow $\beta\text{-SrGe}_2\text{O}_5$ single crystals, 100 mg SrGeO_3 (monoclinic, $C2/c$) powder was mixed in the 1:12 molar ratio with a $\text{SrCl}_2/\text{NaCl}$ flux of the molar composition 8:2. The eutectic point in the $\text{SrCl}_2\text{-NaCl}$ system lies at 544 °C and 53 mol% SrCl_2 .⁹ SrCl_2 and NaCl were dehydrated at 350 °C, and the powder mixture was filled into a Au capsule, pressed and inserted into a NaCl (10 wt.% ZrO_2) cell with a carbon heater. Using a belt-type high-pressure apparatus, a 5 GPa pressure was applied and the specimen was annealed at 1100 °C for 4 hours, then slowly cooled down to 800 °C within 18 h, at which temperature the heater was turned off and the specimen was water-cooled to room temperature. The flux was washed out with deionized water.

We performed single crystal X-ray diffraction (XRD) measurement of the $\beta\text{-SrGe}_2\text{O}_5$ sample at room temperature on a curved type imaging plate diffractometer (Rigaku R-AXIS RAPID II) with graphite monochromatic $\text{Mo-K}\alpha$ radiation. The intensity data was collected by the Rapid Auto program (Rigaku). The initial structural model (orthorhombic, $Pmna$), named $\beta\text{-SrGe}_2\text{O}_5$, was suggested based on the unit cell dimensions and the reflection data. Internal atomic coordinates and anisotropic displacement parameters for all atoms were then refined according to the full-matrix least-squares method using SHELXL.¹⁰ The Bragg-Brentano powder XRD pattern of ground single crystals was recorded using a Bruker RINT2000 diffractometer with a $\text{Cu K}\alpha$ source.

Undoped $\beta\text{-SrGe}_2\text{O}_5$ and Sb-doped $\beta\text{-Sr}(\text{Ge}_{0.95}\text{Sb}_{0.05})_2\text{O}_5$ polycrystalline pellets were prepared from stoichiometric quantities of SrCO_3 , GeO_2 and Sb_2O_5 , ground and calcined at 950 °C for 12 h. The powder mixture was pressed into a Cu capsule, then sintered at 1000 °C for 2 h at 4 GPa pressure. For optical measurements, the pellet surface was mirror-polished by finishing with 0.3 μm fine-grained foil. The Fourier-transform infrared (FTIR) reflectance spectrum (Bruker Vertex 70v) of the polished $\beta\text{-SrGe}_2\text{O}_5$ and $\beta\text{-Sr}(\text{Ge}_{0.95}\text{Sb}_{0.05})_2\text{O}_5$ pellets were measured from 500-5000 cm^{-1} wavenumber using a Au mirror as a 100% reflectance standard.

Computational Methods

Hybrid DFT calculations using the PBE0 functional¹¹ were performed to obtain the β -SrGe₂O₅ (orthorhombic, *Pnma*) ground state crystal structure, with the ionic forces converged to less than 0.01 eV/Å. We used the projector augmented wave (PAW) method as implemented in the Vienna Ab initio Simulation Package (VASP).^{12,13} The electronic band structure was calculated employing maximally localized Wannier functions,¹⁴ a Γ -centered 4 x 4 x 3 *k*-mesh and a plane wave cutoff energy of 500 eV. We employed the PBE0 functional because it gives a reasonable band gap for related compounds, SrGeO₃ (cubic, *Pm-3m*, $E_g^{\text{calc}} = 2.74$ eV, $E_g^{\text{exp}} = 2.8$ eV) and GeO₂ (tetragonal, *P4₂/mnm*, $E_g^{\text{calc}} = 4.55$ eV, $E_g^{\text{exp}} = 4.68$ eV¹⁵). The frequency-dependent real and imaginary dielectric tensor elements ϵ_x , ϵ_y and ϵ_z were calculated using density functional perturbation theory.¹⁶

Employing DFT, energy calculations of all (meta)stable compounds including the high-pressure polymorphs in the SrO-GeO₂ system were performed for a fixed set of volumes around the equilibrium volume. In each calculation, the unit cell shape was relaxed at the given constant volume. We used variable-cell structure relaxations using the generalized gradient approximation (GGA) and the Perdew-Burke-Ernzerhof (PBE) functional.¹⁷ A maximum *k*-point spacing of 0.3 Å⁻¹ was used.

References

- (1) Shirvinskaya, A. K.; Grebenschikov, R. G.; Toropov, N. A. *Izv. Akad. Nauk SSSR, Neorg. Mater.* **1966**, 2, 332.
- (2) Grebenschikov, R. G.; Shirvinskaya, A. K.; Parfenenkov, V. N.; Shitova, V. I.; Toropov, N. A. *Dokl. Akad. Nauk SSSR* **1967**, 174, 839.
- (3) Nakatsuka, A.; Arima, H.; Ohtaka, O.; Fujiwara, K.; Yoshiasa, A. Crystal Structure of SrGeO₃ in the High-Pressure Perovskite-Type Phase. *Acta Crystallogr. Sect. E* **2015**, 71, 502.

- (4) Nakatsuka, A.; Sugiyama, K.; Ohkawa, M.; Ohtaka, O.; Fujiwara, K.; Yoshiasa, A. A New High-Pressure Strontium Germanate, SrGe₂O₅. *Acta Crystallogr. Sect. C* **2016**, *72*, 716.
- (5) Nemeth, P.; Buseck, P. R.; Leinenweber, K.; Groy, T. L. A New High-Pressure CaGe₂O₅ Polymorph with 5- and 6-Coordinated Germanium. *Am. Mineral.* **2007**, *92*, 441.
- (6) Hummel, R. E. *Electronic Properties of Materials*, 4th ed.; Springer-Verlag New York, 2011.
- (7) Murnaghan, F. D. The Compressibility of Media under Extreme Pressures. *Proc. Natl. Acad. Sci.* **1944**, *30*, 244.
- (8) Wedler, G. *Lehrbuch Der Physikalischen Chemie*, 5th ed.; WILEY-VCH, 2004.
- (9) M. Gasanaliev, A.; I. Rasulov, A.; Yu. Gamataeva, B.; K. Mamedova, A. Phase Complex of a NaCl-KCl-SrCl₂-Sr(NO₃)₂ Four-Component System and the Physicochemical Properties of a Eutectic Mixture. *Russ. J. Phys. Chem. A* **2012**, *86*, 154.
- (10) Sheldrick, G. M. Crystal Structure Refinement with SHELXL. *Acta Crystallogr. Sect. C* **2015**, *71* (1), 3.
- (11) Perdew, J. P.; Ernzerhof, M.; Burke, K. Rationale for Mixing Exact Exchange with Density Functional Approximations. *J. Chem. Phys.* **1996**, *105* (22), 9982.
- (12) Kresse, G.; Furthmüller, J. Efficient Iterative Schemes for Ab Initio Total-Energy Calculations Using a Plane-Wave Basis Set. *Phys. Rev. B* **1996**, *54* (16), 11169.
- (13) Kresse, G.; Joubert, D. From Ultrasoft Pseudopotentials to the Projector Augmented-Wave Method. *Phys. Rev. B* **1999**, *59* (3), 1758.
- (14) Mostofi, A. A.; Yates, J. R.; Lee, Y.-S.; Souza, I.; Vanderbilt, D.; Marzari, N. Wannier90: A Tool for Obtaining Maximally-Localised Wannier Functions. *Comput. Phys. Commun.* **2008**, *178* (9), 685.
- (15) Stapelbroek, M.; Evans, B. D. Exciton Structure in the u.v.-Absorption Edge of Tetragonal GeO₂. *Solid State Commun.* **1978**, *25* (11), 959.
- (16) Gajdoš, M.; Hummer, K.; Kresse, G.; Furthmüller, J.; Bechstedt, F. Linear Optical

Properties in the Projector-Augmented Wave Methodology. *Phys. Rev. B* **2006**, 73 (4), 45112.

- (17) Perdew, J. P.; Burke, K.; Ernzerhof, M. Generalized Gradient Approximation Made Simple. *Phys. Rev. Lett.* **1996**, 77 (18), 3865.